Pergamon

Int. J. Heat Mass Transfer. Vol. 39, No. 4, pp. 831–839, 1996

0017-9310/96 $15.00 + 0.00

0017-9310(95)00141-7

Thermal contact conductance of tool steel and comparison with model

M. R. SRIDHAR and M. M. YOVANOVICH

Microelectronics Heat Transfer Laboratory, Department of Mechanical Engineering, University of Waterloo, Waterloo, Ontario, Canada N2L 3G1

(*Received* 3 *October* 1994 *and in final form* 27 *March* 1995)

Abstract—Thermal contact conductance measurements were made on ground-lapped interfaces of tool steel and they were compared with the recently proposed elastoplastic model. The type of deformation associated with contact conductance measurements of ground-lapped interfaces of untreated tool steel was elastoplastic, whereas heat treated tool steel (HRC = 40 and 58) underwent fully elastic deformation. It is found that the interface equivalent elastic modulus for tool steel and some previous data are higher than the equivalent bulk elastic modulus. Even though the effect of sampling interval on the elastoplastic model is significant, a good comparison between previous data and the model is observed with surface slope obtained from a commercial surface analyser. Simple correlations for the elastoplastic model and a semi-explicit expression to calculate the dimensionless contact pressure are proposed.

1. INTRODUCTION

Heat transfer through interfaces is of interest in microelectronic-chip cooling, heat exchangers and in nuclear engineering. Interface heat transfer is a combination of heat transfer through the contacting micro-asperties as well as through the interstitial medium. The present work is directed towards better understanding of micro-asperity heat transfer. The path through the interstitial medium is eliminated by working in a vacuum environment.

Contact conductance work has been limited to comparing data with either elastic or plastic models [1–4]. The elastoplastic model proposed by Sridhar and Yovanovich [5] enables the comparison of data with both models in dimensionless form on the same plot. Maddren [6] has compared data in dimensional form with both models. However, he did not use an appropriate value of hardness in the plastic model.

In Sridhar and Yovanovich [7] it is seen that (i) some data sets compared well with both the elastic and plastic models, and (ii) some data sets were below the elastic model for which the type of deformation could not be explained. Some of these data sets also did not compare well with the elastoplastic model in Sridhar and Yovanovich [5].

This study is mainly devoted towards addressing these issues. Tool steel is a hard material and it is expected that hardened tool steel interfaces will undergo purely elastic deformation and thus give an insight to discrepancies observed between the zirconium alloy data and the elastic model in refs [5 and 7]. Another important issue often raised in the literature is the effect of sampling interval on the surface slope. This has been investigated in detail in this work.

2. EXPERIMENTAL WORK

A total number of nine cylindrical tool steel (01) specimens were used in the present work. The specimens were classified into three categories: untreated (A), heat treated to HRC = 40 (B) and heat treated to HRC = 58 (C). Three samples were used in each category, i.e. one for thermal conductivity measurements and two for the thermal contact conductance tests. Hence six of the nine specimens were heat treated (B and C).

2.1. *Specimen preparation*

The tool steel (01) material is obtained as a 25.4 mm diameter and 1 m long rod.

2.1.1. *Untreated specimens.* The untreated samples underwent the following procedures before the actual testing:

(1) The specimens were turned to 25 mm diameter and 46 mm long rods.

(2) Six thermocouple holes 0.64 mm diameter and 2.5 mm deep were drilled 5 mm apart. The first hole is 10.5 mm from the upper or the lower surfaces, respectively.

(3) The specimens were then finished to the required length dimension (45 mm).

(4) The 30 gauge type "T" copper–constantan thermocouples were spot-welded into the holes. Mica was placed under the bare junctions to insulate the thermocouples electrically. Then the thermocouple leads were wrapped around the specimen and fastened to the specimen with small metallic strips.

(5) The specimens were cleaned with acetone and stored in a desiccator. Later the specimens were cleaned again before installing in the vacuum chamber.

NOMENCLATURE

A_a apparent contact area [m^2]
c_1, c_2 Vickers correlation coefficients, c_1 [MPa]
d_V Vickers indentation diagonal [μm]
E elastic modulus [MPa]
E' equivalent elastic modulus [MPa] $\equiv [(1-\nu_A^2)/E_A+(1-\nu_B^2)/E_B]^{-1}$
E_c equivalent interface elastic modulus [MPa] $\equiv 1.5\times E'$
E_{rigid} equivalent modulus when one surface is perfectly rigid $\equiv E/(1-\nu^2)$ [MPa]
$f_{ep}(\varepsilon_c^*)$ function used in the elastoplastic model
H_B bulk hardness [MPa]
H_B^* dimensionless bulk hardness $\equiv H_B/3178$
H_e elastic contact hardness [MPa]
H_{ep} elastoplastic contact hardness [MPa]
h_c contact conductance [W (m$^2\cdot$K)$^{-1}$]
k thermal conductivity [W (m$\cdot$K)$^{-1}$]
k_s harmonic mean thermal conductivity, $\equiv 2k_Ak_B/(k_A+k_B)$ [W (m$\cdot$K)$^{-1}$]
m effective mean absolute surface slope $\equiv \sqrt{m_A^2+m_B^2}$ [rad]
P nominal contact pressure [MPa]
R_c thermal contact resistance [K/W]
Q heat transfer rate [W]
$\bar{Q}$ average heat flow rate $\equiv (Q_A+Q_B)/2$ [W]
T_c mean interface temperature [°C].

Greek symbols
ΔT_c effective temperature drop across the interface, °C
ε_c^* non-dimensional contact strain
λ dimensionless surface mean plane separation
ν Poisson's ratio
σ root mean square (rms) surface roughness heights for given surface or surface pair $\equiv \sqrt{\sigma_A^2+\sigma_B^2}$, m.

Subscripts
A, B surfaces A and B
a apparent area
e elastic
p plastic
ep elastoplastic.

Abbreviations
A untreated tool steel (01)
B, C heat treated tool steel (01)
HRC hardness Rockwell "C"
Ni nickel
SS stainless steel
Zr–Nb zirconium alloy with niobium
Zr-4 zirconium alloy.

2.1.2. *Heat treated specimens.* A similar procedure as described above was adopted for the heat treated specimens, except that they were kept 47 mm long initially and that meant that the first thermocouple hole was 11 mm from the upper or lower surfaces. The heat treatment was performed between steps 2 and 3. Initially the specimens were hardened by heating (about 800°C, 15 min) and quenching in oil. After quenching the test pieces were tempered in two sets for 2 h at 543 and 204°C to obtain heat treated specimens B (HRC = 40) and C (HRC = 58), respectively.

2.1.3. *Surface finish.* The thermal contact conductance tests were limited to similar ground-lapped interfaces. The ground surface were prepared using AA60H8V40 smooth grinding wheel as recommended by Nho [3] for hard materials. Lapped surfaces were prepared by mechanical lapping. The flatness deviation of the samples were found to be less than 0.3 μm. They were checked using a Krypton 86 monochromatic light source and an optical flat.

2.2. *Experimental setup*

The experimental setup used here is identical to that used by Hegazy [2], and followed by Song [8] and Nho [3]. A detailed description of the setup can be found in Nho [3]. The test column is enclosed by a Pyrex bell jar and a base plate (Fig. 1). The test column consists of the heater block, the heat meter, the upper and lower test specimens, the heat sink and the load cell. The gas pressure within the bell jar is controlled by a vacuum system which is a combination of a mechanical pump connected in series with an oil diffusion pump. A vacuum level lower than 10^{-5} torr could be achieved. The heater consists of two pencil-type heaters embedded into a brass block. A closed loop thermobath is used to cool the aluminum cold plate. The load is applied to the test column with the aid of a diaphram-type air cylinder. A calibrated load cell is used to measure the applied load. The mechanical loads, heater levels and data acquisition were controlled with a PC.

2.3. *Thermal conductivity and contact conductance of tool steel*

The experimental thermal contact conductance in a vacuum environment is defined as

$$h_c=\frac{1}{R_cA_a}=\frac{\bar{Q}/A_a}{\Delta T_c} \quad (1)$$

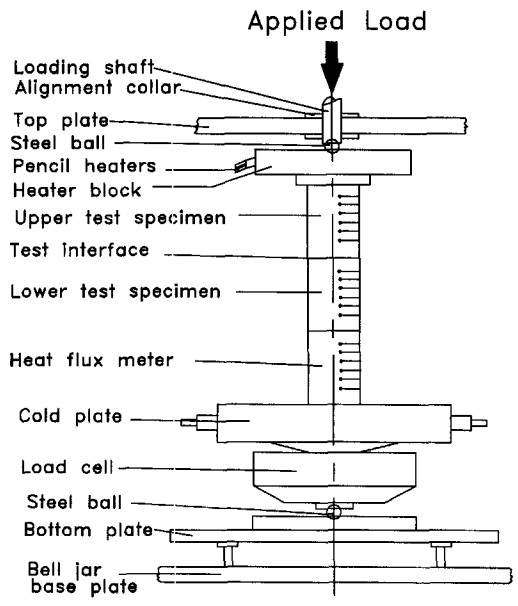

Fig. 1. Experimental setup.

where $\bar{Q}$ is an average heat flow rate through the joint and ΔT_c is the temperature drop across the interface and A_a is the apparent contact area. This average heat flow rate $\bar{Q}$ is determined from an average of two heat flow rates Q_A, Q_B passing through the upper and lower specimens: $\bar{Q} = (Q_A + Q_B)/2$. The flow rates Q_A and Q_B are estimated from the measured least-square fits of the temperatures along each specimen.

$$Q_A = q_A \cdot A_a = -k_A \cdot A_a \cdot \left.\frac{dT}{dx}\right|_A$$

$$Q_B = q_B \cdot A_a = -k_B \cdot A_a \cdot \left.\frac{dT}{dx}\right|_B$$

where k_A, k_B are the measured thermal conductivities of the upper and lower specimens, $(dT/dx)_A$ and $(dT/dx)_A$ are temperature gradients obtained using least-squares-fit of the measured thermocouple temperatures.

The thermal conductivities of untreated and heat treated tool steel specimens (A, B and C) were measured from three separate vacuum tests using armco iron heat flux meters. The thermal conductivity of armco iron is widely known [3]:

$$k[W(m \cdot K)^{-1}] = 74.6 - 0.069T(°C).$$

This empirical correlation is valid for a temperature range from 20 to 300 (°C) with a maximum error of 1.5%. The test sample is placed between the two armco iron heat meters and the vacuum is drawn. The average heat flow rate is estimated using the heat meters and knowing the temperature gradient in the sample, the conductivity was estimated at different temperature levels. All thermal conductivities were assigned to the mid-plane temperature. It is interesting to see that samples A, B and C had distinctly different conductivities:

A $k[W(m \cdot K)^{-1}] = 51.77 - 0.0202T(°C)$

$29 < T < 196$

B $k[W(m \cdot K)^{-1}] = 47.71 - 0.0240T(°C)$

$29 < T < 194$

C $k[W(m \cdot K)^{-1}] = 35.32 - 0.0063T(°C)$

$33 < T < 199.$

The correlations show that they are weak functions of temperature. The untreated tool steel (A) had the highest conductivity and the heat treated ones (B and C) with the hardest sample (C, HRC = 58) having the lowest. The RMS % errors between the three correlations and data were around 1.0%. The maximum % errors for A, B and C were 1.5, −2.8 and −2.4%, respectively.

The average interface temperature T_c for similar metal pairs ($k_A = k_B$) tested in the present investigation is the mean of the extrapolated surface temperatures (T_A, T_B) given by $T_c = (T_A + T_B)/2$.

2.4. *Surface characterization of tool steel*

Surface characterization of tool steel involves measurements of surface microhardness and surface roughness of the ground-lapped interfaces used in the present work. The hardness measurements were made on lapped surfaces whereas the roughness measurements were made both on lapped as well as ground surfaces.

2.4.1. *Surface microhardness.* Vickers microhardness variation with indentation size for tool steel (01) was examined in Sridhar and Yovanovich [9] for different values of the bulk hardness. The bulk hardness was varied by heat treatment. The plots of Vickers microhardness vs indentation size were correlated with a simple power law relation: $H_V = c_1 d_V^{c_2}$. The Vickers correlation coefficients c_1 and c_2 were found to have definite relationship with the Brinell hardness. Two methods of correlating the coefficients c_1 and c_2 and the Brinell hardness H_B were proposed. The second method was generally superior and it is given by:

$$\frac{c_1}{3178} = [4.0 - 5.77(H_B^*) + 4.0(H_B^*)^2 - 0.61(H_B^*)^3], \quad (2)$$

where $H_B^* = H_B/3178$, and

$$c_2 = -0.370 + 0.442\left(\frac{H_B}{c_1}\right). \quad (3)$$

These correlations are valid for Brinell hardness and Rockwell hardness ranges of 1300–7600 MPa and 19–66, respectively. These correlations also cover a wide range of materials (SS304, Ni200, two zirconium

alloys, titanium alloy, and untreated and heat treated tool steel (01)).

2.4.2. *Surface roughness.* In the present work thermal contact conductances were measured for ground-lapped interfaces of as received tool steel (A), and two other heat treated tool steels (B and C). The surface roughness and slopes of the ground and lapped surfaces were measured using Taylor Hobson Talysurf-5. The experimental procedure employed here closely follows the one developed by Hegazy [2] and followed by Song [8] and Nho [3]. It was found for the present work on tool steel that the surface heights and slopes had near-Gaussian distribution [10].

It is believed [11, 12] that the surface slope is strongly dependent on sampling interval. However, McWaid [4] has reported very little variation of slope with sampling interval. In the present work a large variation of slope with sampling interval was observed (Fig. 2) as the sampling interval is varied from 0.84 to 70 μm. In Fig. 2 it can be seen that the rms roughness is invariant for both ground and lapped surfaces. Now the question is, which is the correct sampling interval at which the slope measurements are to be made? This issue has been raised by authors such as Thomas [11], Bhushan *et al.* [12], Greenwood [13], Johnson [14] and others. None of them offered a solution and this problem remains unresolved.

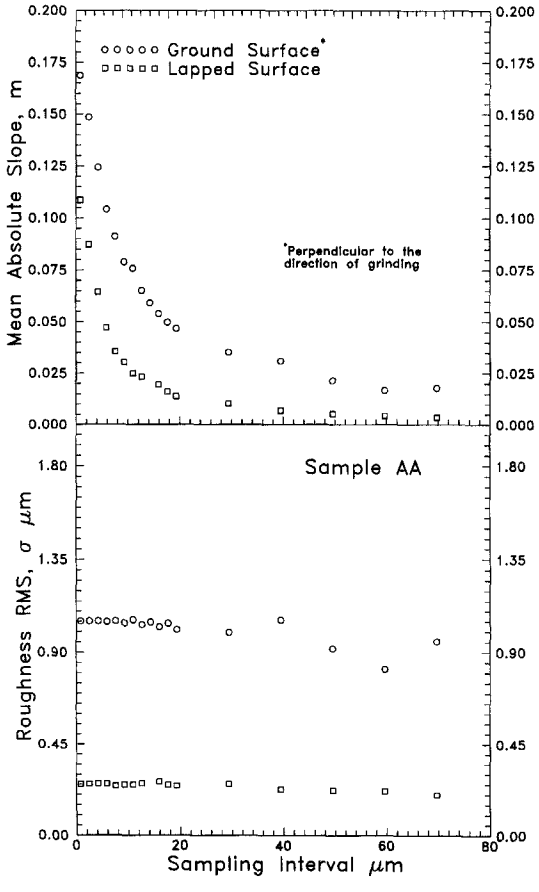

Fig. 2. Effect of sampling interval on surface parameters.

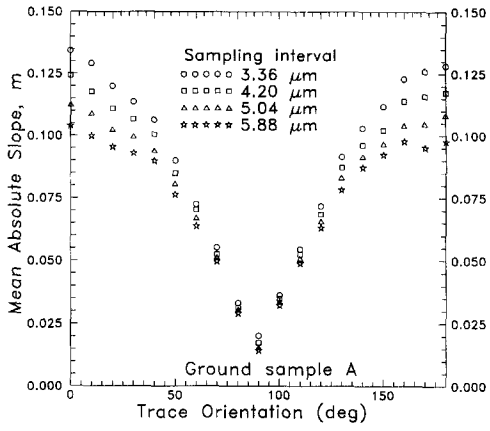

Fig. 3. Plot of surface slope against trace orientation at four different sampling intervals.

An attempt is made in the present work to arrive at a particular value of sampling interval for the ground-lapped surfaces. The stylus used in the present profilometer (Talysurf-5) has a tip radius of 1.5 μm. It is clear that in order to have independent samples any sampling interval greater than the diameter of the stylus tip (i.e. 3 μm) is valid. Therefore, the ground and lapped surfaces were characterized at four different sampling intervals, i.e. 3.4, 4.2, 5.0 and 5.9 μm. A ground surface is an anisotropic surface for which the surface slope varies with direction. The measurements were made on each ground surface at 10° increments starting from the line perpendicular to the grinding direction to 180°. A total of 19 traces were recorded for each ground surface. For lapped surfaces, two traces perpendicular to each other were taken. Since the specimens were 25 mm in diameter a trace length 10 mm is selected. A cutoff of 0.8 mm is used (recommended by ISO [15]). Figure 3 shows a typical plot of mean absolute slope against trace orientation for a ground surface of untreated tool steel (A) at four different sampling intervals. It should be noted that the smaller the sampling interval, the higher is the value of the slope at each trace orientation.

The suggestion of Nho [3] that an anisotropic surface can be defined as an equivalent isotropic surface is used here, i.e. by using a geometric mean of the maximum and minimum surface slopes. Hence a ground-lapped interface can be reduced to an equivalent isotropic interface. If we define σ_A, $m_{\mathrm{mx}A}$ and $m_{\mathrm{mn}A}$ as rms roughness, maximum and minimum mean absolute slopes of the ground surface with σ_B and m_B being the rms roughness and mean absolute slope of the lapped surface, then for ground-lapped surface pair we have:

Equivalent slope for ground surface

$$m_{\mathrm{gr}} = \sqrt{m_{\mathrm{mx}A} \cdot m_{\mathrm{mn}A}}. \tag{4}$$

Equivalent roughness for the surface pair

$$\sigma = \sqrt{\sigma_A^2 + \sigma_B^2}. \tag{5}$$

Table 1. Equivalent isotropic surface properties of ground-lapped interfaces

Surface pair	Sampling interval [μm]	rms roughness σ [μm]	Mean absolute slope m [rad]	σ/m [μm]
AA	3.36	0.981	0.0892	11.0
	4.20	0.981	0.0773	12.7
	5.04	0.980	0.0670	14.6
	5.88	0.982	0.0599	16.4
BB	3.36	0.595	0.0475	12.5
	4.20	0.594	0.0429	13.9
	5.04	0.596	0.0384	15.5
	5.88	0.594	0.0349	17.0
CC	3.36	0.588	0.0450	13.1
	4.20	0.589	0.0405	14.5
	5.04	0.588	0.0366	16.1
	5.88	0.587	0.0340	17.3

Equivalent slope for the surface pair

$$m = \sqrt{m_{gr}^2 + m_B^2}. \tag{6}$$

Table 1 shows values of equivalent rms surface roughness, σ (μm) and equivalent surface slope m of the three similar metal pairs of tool steel A, B and C obtained at four different sampling intervals.

3. CORRELATIONS FOR ELASTOPLASTIC MODEL

The elastoplastic contact conductance model was proposed in Ref. [5] for isotropic conforming rough surfaces. This model is based on surface and thermal models by Cooper, Mikic and Yovanovich (CMY) [16], but it differs in the deformation aspects of the CMY model. The model incorporates the simple elastoplastic model for sphere-flat contacts proposed in Ref. [10]. This model [5] covers the three deformation regimes: elastic; elastoplastic; and fully plastic. The dimensionless contact conductance $C_c = (\sigma h_c)/(m k_s)$, where

$$\sigma = \sqrt{\sigma_A^2 + \sigma_B^2}, \quad m = \sqrt{m_A^2 + m_B^2},$$
$$k_s = (2k_A k_B)/(k_A + k_B)$$

are the rms roughness, mean absolute slope and harmonic mean thermal conductivity of the surface pair:

$$C_c = \frac{1}{2\sqrt{2\pi}} \frac{\sqrt{f_{ep}(\varepsilon_c^*)} \cdot \exp(-\lambda^2/2)}{\left[1 - \sqrt{\frac{f_{ep}(\varepsilon_c^*)}{2}} \operatorname{erfc}(\lambda/\sqrt{2})\right]^{1.5}},$$
$$\lambda = \sqrt{2} \operatorname{erfc}^{-1}\left(\frac{1}{f_{ep}(\varepsilon_c^*)} \cdot \frac{2P}{H_{ep}}\right), \tag{7}$$

where $f_{ep}(\varepsilon_c^*)$ is an elastoplastic function which depends on the non-dimensional contact strain ε_c^*, P is the applied pressure and H_{ep} is the elastoplastic hardness of the softer material in contact. The

Table 2. Elastoplastic model correlations

Correlation	Equation no.	Range of validity
$C_c = 1.54\left(\frac{P}{H_{ep}}\right)^{0.94}$	(8)	$0 < \varepsilon_c^* < 5$
$C_c = 1.245 b_1(\varepsilon_c^*)^a \cdot \left(\frac{P}{H_{ep}}\right)^{0.948 b_2(\varepsilon_c^*)^b}$	(9)	$5 < \varepsilon_c^* < 400$
$C_c = 1.25\left(\frac{P}{H_{ep}}\right)^{0.95}$	(10)	$400 < \varepsilon_c^* < \infty$

$^a b_1(\varepsilon_c^*) = \left(1 + \frac{46690.2}{\varepsilon_c^{*2.48}}\right)^{1/30}$. $^b b_2(\varepsilon_c^*) = \left(\frac{1}{1 + \frac{2086.9}{\varepsilon_c^{*1.842}}}\right)^{1/600}$.

elasoplastic function f_{ep} can take values from 0.5 to 1.0 depending on the type of deformation.

A simple power law correlation of equation (7) was proposed for different values of the non-dimensional strain ε_c^*. It was found that when $\varepsilon_c^* \leqslant 5$ the elasto-plastic model coincided with the Mikic [17] elastic model and when $\varepsilon_c^* \geqslant 400$, it coincided with the CMY [16] plastic model. The correlations were generated similar to the way Devaal [18] correlated his anistropic plastic model, i.e. power law correlations of the form $a(P/H_{ep})^b$ were generated for different values of ε_c^*. The elastoplastic function f_{ep} varied from 0.5 to 0.94 as ε_c^* is varied from 5 to 100 and 0.94 to $\simeq 1.0$ as ε_c^* varied from 100 to 400. Correlations were generated for ε_c^* intervals of 5 in the range 5–100 and intervals 20 in the range 100–400. The constants (a and b) generated at different values of ε_c^* were recorrelated to obtain $b_1(\varepsilon_c^*)$ and $b_2(\varepsilon_c^*)$. The correlations for the elastoplastic model are summarized in Table 2. The correlations are valid for a P/H_{ep} range of 10^{-6} to 2×10^{-2}. The rms % errors between the actual model and the correlations [equation (8) and equation (10) in Table 2] for the above mentioned P/H_{ep} range were 1.4 and 1.6%, respectively. The correlation, equation (9), recorded a maximum rms % error of 1.6% at $\varepsilon_c^* = 5$.

4. SEMI-EXPLICIT EXPRESSION TO CALCULATE APPROPRIATE VALUE OF P/H_{ep}

An iterative procedure was developed in ref. [5] to calculate the appropriate value of the dimensionless contact pressure P/H_{ep}. The equations were combined in ref. [10] to obtain the semi-explicit expression

$$\frac{P}{H_{ep}} = \left[\frac{0.9272P}{c_1\left(1.62\frac{\sigma}{m}f_{ep}^{0.429}\right)^{c_2}}\right]^{\frac{1}{1+0.071c_2}}, \quad (11)$$

where the elastoplastic function f_{ep} is given by

$$f_{ep} = \frac{\left[1+\left(\frac{6.5}{4.61\sqrt{(1/P^* \cdot P/H_{ep})^2-2}}\right)^2\right]^{1/2}}{\left[1+\left(\frac{13.0}{4.61\sqrt{(1/P^* \cdot P/H_{ep})^2-2}}\right)^{1.2}\right]^{1/1.2}}, \quad (12)$$

where $P^* = P/(E' \cdot m)$, E' and m are the equivalent elastic modulus and mean absolute surface slope for the surface pair. In order to obtain the appropriate value of P/H_{ep} for a particular applied pressure P, equations (11) and (12) have to be solved iteratively until the assumed value of f_{ep} in equation (11) coincides with the value calculated in equation (12). Since f_{ep} is known to lie between 0.5 and 1.0 the above set of equations converge very quickly. Equation (11) closely resembles the explicit expression obtained by Song and Yovanovich [19] for isotropic surface pairs undergoing fully plastic deformation.

5. TEST RESULTS AND COMPARISONS WITH PROPOSED MODEL

Thermal contact conductance tests were performed for three similar metal pairs (i.e. AA, BB and CC), ground-lapped interfaces, of tool steel (01). The directional effect was also examined, i.e. heat flow from ground to lapped surfaces as well as from lapped to ground surfaces. Directional effect was not observed for the similar metal pairs of tool steel tested here.

5.1. *Experimental uncertainty*

A detailed experimental uncertainty analysis on the tool steel data is available in ref. [10]. The uncertainties in C_c, P/H_c and P/H_{ep} are ± 18.4, ± 15.6 and $\pm 17.1\%$, respectively.

5.2. *Data reduction*

The first step in data reduction is to compare the data with the Mikic [17] elastic model to confirm the type of deformation. This model has been presented in refs [5, 7]. The contact conductance h_c was calculated using equation (1). The dimensionless contact conductance is determined by multiplying h_c by $\sigma/(mk_s)$. Since it is known that the mean absolute slope m is a function of sampling interval (see Table 1), a sampling interval of 3.36 μm was arbitrarily chosen. The harmonic mean conductivity k_s was determined for each thermal measurement.

The x-axis, i.e. dimensionless elastic contact pressure is given by $P/H_c = \sqrt{2}P/(E'm)$. For similar metals in contact the equivalent elastic modulus is given by $E' = E/[2(1-\nu^2)]$, where E is the elastic modulus of the material. The *ASM Handbook* [20] value of elastic modulus at room temperature for tool steel is $E = 200$ GPa. The *ASM Handbook* [20] also reports a value of $E = 180$ GPa at 260°C. The temperature range in the present test is 73–121°C, which means that the elastic modulus is between 192–196 GPa. Since this value is well within the uncertainty of selecting the elastic modulus from the handbook, the room temperature modulus was used. In the earlier work [5, 7] a single value of $E = 96$ GPa was used for both zirconium alloys. It is known from the experimental work of Rosinger *et al.* [21] that the modulus of elasticity varies with temperature. From their empirical correlations it is concluded that a single value of $E = 87.8$ GPa which lies well within $\pm 2.5\%$ of the correct value for both the zirconium alloys for the entire temperature range (107–179°C) is most appropriate. This is well within the uncertainty of picking the property from the handbook.

Figure 4 shows a comparison of the three data sets (AA, BB and CC) for both directions of heat flow with the Mikic elastic model. Since Zr–Nb and Zr-4 data from Hegazy [2] compared well with BB and CC sets, they have also been included. It is seen from the comparison that the data set AA is undergoing a significant plastic deformation. The other sets BB and CC along with Zr–Nb and Zr-4 data lie below the

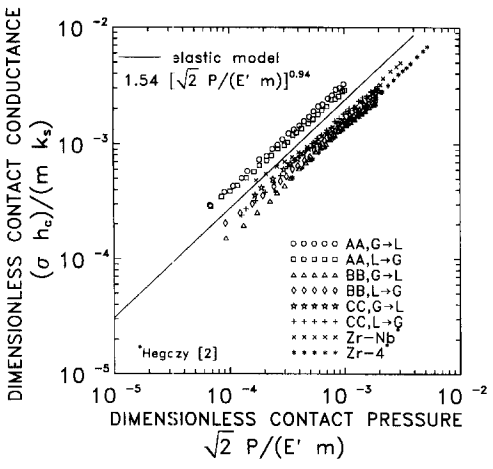

Fig. 4. Comparison of tool steel (01) and zirconium alloy data with elastic model.

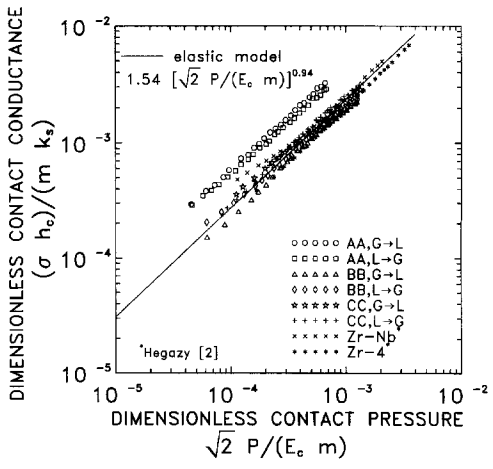

Fig. 5. Comparison of tool steel (01) and zirconium alloy data ($E' = E_c$) with elastic model.

Mikic elastic model. Directional effect is not observed for all the three sets of tool steel data.

The surface slope m appears in the denominator of both x and y axis. This means that whatever value of m is used to reduce the data, the data will always lie at the same level below the elastic model. Hence, it is clear that the reason that the data lies below the elastic model is due to using an incorrect value of E'. Tool steel data are from anisotropic interfaces (ground-lapped) which are reduced as equivalent isotropic interfaces and are being compared to an isotropic model. The question arises whether the harder tool steel data (BB and CC) are below the model because of this. It should be noted from Devaal's [18] work that anisotropy is supposed to move the data in the opposite direction and is an insignificant aspect of contact conductance modelling (see Nho [3]).

The appropriate value of the equivalent elastic modulus E_c seems to be equal to $1.5 \times E'$. This happens to be the mean of the two limits, i.e. E' and E_{rigid}, where E_{rigid} is the equivalent elastic modulus when one of the contacting surface is considered perfectly rigid.

Figure 5 shows a comparison of data sets BB, CC, Zr–Nb and Zr-4 with the Mikic elastic model with E' replaced by $E_c = 1.5 \times E'$. The comparison is quite good with the overall rms difference for the four data sets being 14.7%. It should be noted that Zr–Nb data have a significant low load deviation.

The next step is to reduce the data set AA, with the elastic modulus E_c, and compare it with the elastoplastic model for different values of sampling intervals shown in Table 1. The comparisons are summarized in Table 3. The first and the second column list the sampling interval and non-dimensional contact strain ε_c^*. The rms % differences between elastoplastic model and data (rms_{ep}), elastoplastic model and data with first two data points removed (rms_{ep-2}), and elastic model and data are reported in columns 3, 4 and 5, respectively. The comparison between data and model with first two data points removed was made to ensure that there was negligible low load deviation as previously reported by Hegazy [2] and Nho [3].

It is clear from Table 3 that the most suitable value of sampling interval is about 4.20 μm where the data for both directions of heat flow agree well with the model. However, the comparison seems to be reasonable in the sampling interval range of 3.36–5.04 μm. There is one value of the sampling interval where the rms % difference is the smallest and if the sampling interval is increased or decreased below this value the rms % difference increases. It can also be seen from column 5 of Table 3 that the comparison with data and elastic model is almost independent of the sampling interval as discussed before. Figure 6 shows the comparison of the elastoplastic model ($\varepsilon_c^* = 14.2$) with data set AA reduced using the sampling interval of 4.2 μm.

It should also be noted that with a value of $f_{ep} = 0.5$

Table 3. Comparison of tool steel AA data with elastoplastic model

Sampling interval [μm]	ε_c^*	rms_{ep}[a] % difference $G \to L$	$L \to G$	rms_{ep-2}[b] %difference $G \to L$	$L \to G$	rms_e[c] % difference $G \to L$	$L \to G$
3.36	16.3	6.9	16.0	7.1	16.7	115.4	93.9
4.20	14.2	7.3	8.9	6.0	8.7	117.0	95.5
5.04	12.3	17.4	9.0	16.1	6.6	119.0	97.0
5.88	11.0	27.1	16.0	25.7	13.4	120.8	98.7

[a] Data and ep model; [b] see text; [c] data and e model.

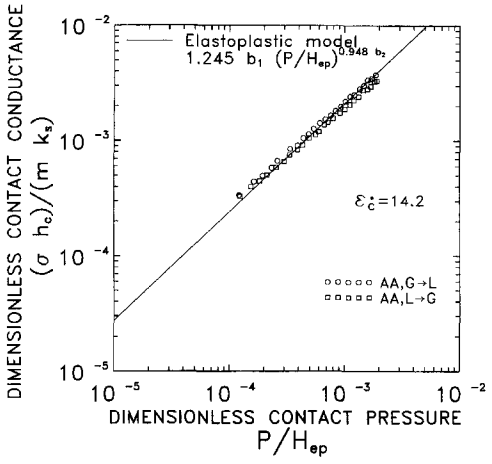

Fig. 6. Comparison of data set AA with elastoplastic model.

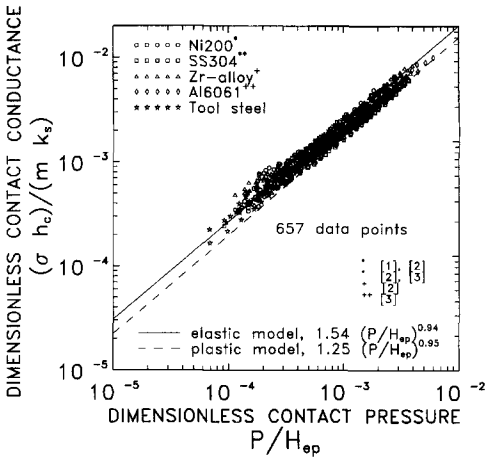

Fig. 8. Comparison of previous and present data with elastic and plastic models.

in equation (11) will not necessarily be equal to the dimensionless elastic contact pressure, i.e. $P/H_e = \sqrt{2}P/(E'm)$, given by the Mikic elastic model [10]. This is because Vickers correlation coefficients in equation (11) are based on tests performed with a diamond pyramidal indenter and not with a spherical indenter as it should be. A pyramidal indenter produces geometrically similar indentations irrespective of the applied load, which means that the type of deformation does not change with load. However, a pyramidal indenter is a good approximation to a spherical indenter in the elastoplastic and fully plastic regime [14].

Figure 7 shows a comparson of the two asymptotic elastic and plastic models with the tool steel data sets AA, BB and CC. A sampling interval of 4.2 μm was used for data sets BB and CC which undergo fully elastic deformation. A good comparison is observed between the data and the two asymptotic models.

The choice of the elastic modulus $E_c = 1.5 \times E'$ is arbitrary. To validate this choice it was decided to reduce available data with this elastic modulus and compare it with the proposed model. However, the choice of data is limited to similar metal pairs of which one surface is lapped.

Figure 8 shows a comparison of all data which have one surface lapped compared with the two models. The comparison is quite good with 657 data points. It should be noted that 511 data points out of the 657 points were reduced using a fixed surface slope. In Fig. 8, Ni200 data includes bead blasted-lapped interfaces from Antonetti [1], Hegazy [2] and ground-lapped interfaces from Nho [3]. The SS304 data includes bead blasted-lapped interfaces from Hegazy [2] and ground-lapped interfaces Nho [3]. The Zr-alloy data includes bead blasted-lapped interfaces from Hegazy [2] and ground-lapped interfaces of Al6061 are from Nho [3]. The ground-lapped interfaces include both directions of heat flow. The comparison of all these data sets with the model is quite good indicating the merit of using the elastic and the elastoplastic model for data reduction.

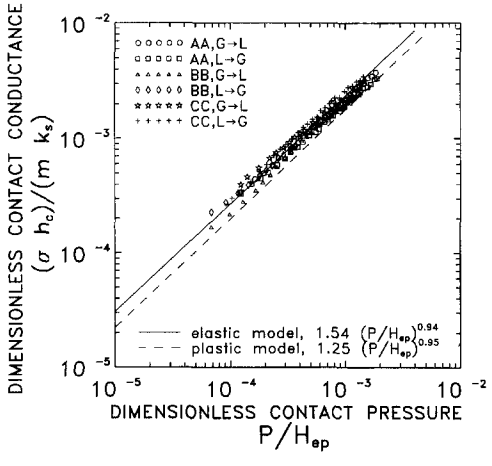

Fig. 7. Comparison of present tool steel data with elastic and plastic models.

6. SUMMARY AND CONCLUSIONS

Thermal contact conductance measurements of ground-lapped interfaces of tool steel revealed that untreated tool steel underwent elastoplastic deformation, while two other heat treated pairs (HRC = 40 and 58) underwent fully elastic deformation. The results from elastically deforming pairs came together on a dimensionless plot, but are below the original Mikic [17] elastic model. When a value of equivalent elastic modulus $E_c = 1.5 \times E'$ is used, the data agrees well with the Mikic elastic model. Even though this choice is arbitrary, it seems to work well for 657 data points from Antonetti [1], Hegazy [2], Nho [3], and the present tool steel data. Future experimental work on hard materials should address this issue to confirm what was observed with tool steel and the zirconium alloys.

The elastic model is almost independent of the

surface slope m, irrespective of the value of m the % difference between the model and the data remains more or less the same (see Table 3). The surface slope is an important parameter for the elastoplastic model. The comparison between data and the model can be improved if an appropriate value of surface slope is used (see Table 3). Suppose a data set undergoing elastoplastic deformation is reduced using the elastic model, rms difference between the model and the data can be as high as 832% (Ni200, $\sigma/m = 24.6\ \mu$m). The maximum rms difference between data and model using a Talysurf value for the surface slope is 34.6% (SS304, $G \rightarrow L$, Nho [3]). It is clear that the most important aspect of thermal contact conductance data reduction is not the surface slope, but the usage of the appropriate value of microhardness.

The elastoplastic function f_{ep}, in equation (11) varies from 0.5 to 1.0. Suppose f_{ep} is fixed at 0.75, the maximum error in f_{ep} is $\pm 33\%$. Since f_{ep} is raised to a fractional power $(0.429 \cdot c_2)$ it has a marginal effect on P/H_{ep}. The error is of the order of $\pm 5.0\%$ for a maximum value $c_2 = -0.28$. The new simplified explicit expression is given by

$$\frac{P}{H_{ep}} = \left[\frac{0.9272P}{c_1 \left(1.43 \frac{\sigma}{m}\right)^{c_2}} \right]^{\frac{1}{1+0.071c_2}}. \qquad (13)$$

It is known from this work that equation (11) does not necessarily equal to (see ref. [10]) the dimensionless elastic contact pressure when f_{ep} is set equal to 0.5. Therefore it is recommended that both the elastic as well as the elastoplastic model be used for data reduction. The first step would be to compare the data with the Mikic elastic model with $E' = E_c$. If significant plastic deformation is observed (i.e. data well above the elastic model on a dimensionless plot), then the elastoplastic model must be used for data reduction. Equation (13) can be used in all cases as a good approximation for equation (11) provided c_2 is not much larger than $|-0.28|$.

Low load deviation of data from the model, which is observed in the results of Hegazy [2], Nho [3] and McWaid [4], is not observed in tool steel data. Most probably this has something to do with the way the power (heat) is applied to the experimental system (i.e. to the heat source). In the present work nearly 8 h were devoted to bringing the system from room temperature to the appropriate temperature level.

Acknowledgements—The authors acknowledge the support of the Natural Science and Engineering Research Council of Canada under grant A7445. The authors would like to thank Mr A. Hodgson and Mr B. Vogel for preparing test specimens.

REFERENCES

1. V. W. Antonetti. On the use of metallic coatings to enhance thermal contact conductance Ph.D. Thesis, University of Waterloo, Waterloo, Ontario (1983).
2. A. A. Hegazy, Thermal joint conductance of conforming rough surfaces, Ph.D. Thesis, University of Waterloo, Waterloo, Ontario (1985).
3. K. M. Nho, Experimental investigation of heat flow rate and directional effect on contact conductance of anisotropic ground/lapped interfaces, Ph.D. Thesis, University of Waterloo, Waterloo, Ontario (1990).
4. T. H. McWaid, Thermal contact resistance across pressed metal contact in a vacuum environment, Ph.D. Thesis, University of California, Santa Barbara, CA (1990).
5. M. R. Sridhar and M. M. Yovanovich, Elastoplastic contact conductance model for isotropic conforming rough surfaces and comparison with experiments, Thermal phenomena at molecular and microscales and in cryogenic infrared detectors. *Proceedings of the 6th AIAA/ASME Thermophysics and Heat Transfer Conference*, Colorado Springs, CO, 1994, HTD-Vol 277, *ASME. J. Heat Transfer* (in press).
6. J. Maddren, Thermal contact resistance of bolted joints at cryogenic temperatures, Ph.D. Thesis, University of California, Santa Barbara, CA (1994).
7. M. R. Sridhar and M. M. Yovanovich, Review of elastic and plastic thermal contact conductance models: comparison with experiment, *J. Thermophys. Heat Transfer* **8,** 633–640 (1994).
8. S. Song, Analytical and experimental study of heat transfer through gas layers of contact interfaces, Ph.D. Thesis, University of Waterloo, Waterloo, Ontario (1988).
9. M. R. Sridhar and M. M. Yovanovich, Empirical methods to predict Vickers micro-hardness *Wear* (in press).
10. M. R. Sridhar, Elastoplastic models for sphere-flat and conforming rough surface applications, Ph.D. Thesis, University of Waterloo, Ontario (1994).
11. T. R. Thomas, *Rough Surfaces*. Longman, London (1982).
12. B. Bhushan, J. C. Wyant and J. Meiling, A new three-dimensional non-contact digital optical profiler, *Wear* **122,** 301–312 (1988).
13. J. A. Greenwood, A unified theory of surface roughness, *Proc. R. Soc. Lond.* **A 393,** 133–157 (1984).
14. K. L. Johnson, *Contact Mechanics*. Cambridge University Press, Cambridge (1985).
15. *ISO Standards Handbook* 33, Applied Metrology—Limits, Fits and Surface Properties (1988).
16. M. G. Cooper, B. B. Mikic and M. M. Yovanovich, Thermal contact conductance, *Int. J. Heat Mass Transfer* **12,** 279–300 (1969).
17. B. B. Mikic, Thermal contact conductance; theoretical considerations, *Int. J. Heat Mass Transfer* **17,** 205–214 (1974).
18. J. W. Devaal, Thermal joint conductance of surfaces prepared by grinding, Ph.D. Thesis, University of Waterloo, Waterloo, Ontario (1988).
19. S. Song and M. M. Yovanovich, Relative contact pressure: dependence on surface roughness and Vickers microhardness, *AIAA J. Thermophys. Heat Transfer* **2,** 43–47 (1988).
20. *Metals Handbook*, ninth Edn, Vol. 3, Properties and Selection: Stainless Steels, Tool Materials and Special Purpose Metals. American Society for Metals, Metals Park, OH (1980).
21. H. R. Rosinger, I. G. Ritchie and A. J. Shillinglaw, Young's modulus of crystal bar zirconium and zirconium alloys (Zircaloy-2, Zircaloy-4, Zirconium-2.5 wt% Niobium) to 1000 K, AECL limited, Whiteshell Nuclear Research Establishment, Pinawa, Manitoba, (1975).